Available online at www.sciencedirect.com
SCIENCE DIRECT
Polymer 47 (2006) 5919–5928
polymer
www.elsevier.com/locate/polymer

Low frequency ac conduction and dielectric relaxation behavior of solution grown and uniaxially stretched poly(vinylidene fluoride) films

Ramadhar Singh [a,*], Jitendra Kumar [a], Rajiv K. Singh [a], Amarjeet Kaur [b], R.D.P. Sinha [c], N.P. Gupta [d]

[a] *Polymeric Devices Group, National Physical Laboratory, Dr. K.S. Krishnan Marg, New Delhi 110 012, India*
[b] *Department of Physics and Astrophysics, University of Delhi, New Delhi 110 007, India*
[c] *Department of Physics, S.R.K. Goenka College, Sitamarhi 843 302, India*
[d] *Department of Physics, J.V. Jain College, Saharanpur 247 001, India*

Received 4 October 2005; received in revised form 9 June 2006; accepted 10 June 2006
Available online 30 June 2006

Abstract

The measurements of ac conductivity [$\sigma_m(\omega)$], dielectric constant [$\varepsilon'(\omega)$] and loss [$\varepsilon''(\omega)$] have been performed on solution grown (thickness ~85 μm) and uniaxially stretched (thickness ~25, 45 and 80 μm) films of poly(vinylidene fluoride) (PVDF) in the frequency range 0.1 kHz–10 MHz and in the temperature range 77–400 K. The $\sigma_m(\omega)$ can be described by the relation $\sigma(\omega) = A\omega^s$, where s is close to unity and decreases with increase in temperature. Three relaxations, observed in the present investigation, have been designated as the α_c-, the α_a- and the β-relaxations appearing from high temperature side to the low temperature side. The α_c-relaxation could not be observed in the case of uniaxially stretched poly(vinylidene fluoride) films. The α_c- and α_a-relaxations are associated with the molecular motions in the crystalline regions and micro-Brownian motion in the amorphous regions of the main polymer chain, respectively, whereas the β-relaxation is attributed to the rotation of side group dipoles or to the local oscillations of the frozen main polymer chain.

Keywords: Uniaxially stretched poly(vinylidene fluoride) films; ac Conductivity; Dielectric relaxation

1. Introduction

The study of dielectric relaxation behavior as a function of temperature and frequency has revealed two or three types of relaxation processes in polymeric materials, namely; α, β, γ, respectively, appearing from high temperature side to the low temperature side and from low frequency side to the high frequency side [1]. The α-relaxation or the primary relaxation process is attributed to the rotation of dipoles from one quasi-stable state to another in which the diffusional motion of the segment occurs. The β-relaxation is associated with the partial orientation of the dipoles in the range of local environments where the large-scale rearrangement of the main chain is frozen. In the recent years, the field of ferroelectric polymers has become an interesting part of research partly due to their piezoelectric behavior responsible for making electromechanical transducers and partly because they exhibit interesting molecular processes associated with various phenomena such as ferroelectric to paraelectric phase transition and polarization switching, etc. [2–8]. After the discovery of piezoelectricity in poly(vinylidene fluoride) (PVDF) [5,9], the interest has been generated for its piezoelectric and pyroelectric applications. The molecular vibrations of the α, β, γ phases of PVDF have been investigated earlier [10]. The morphology and phase transition as well as the effect of crystalline phase, orientation and temperature on dielectric properties of

* Corresponding author. Tel.: +91 11 25742610; fax: +91 11 25726938.
E-mail address: ramadhar@mail.nplindia.ernet.in (R. Singh).

0032-3861/$ - see front matter © 2006 Elsevier Ltd. All rights reserved.
doi:10.1016/j.polymer.2006.06.023

high melt temperature crystallized PVDF have been reported [8,11,12]. Also the distribution of relaxation times from dielectric spectroscopy, using Monte Carlo simulation, in α-PVDF reveals two relaxation processes, i.e. the α_a-relaxation process associated with glass transition and the α_c-relaxation process due to changes in confirmation in the crystalline region [13]. It is known [14] that PVDF possesses low acoustic impedance having excellent matching with water and human tissues, making this polymer very useful for underwater acoustics and medical imaging applications. Before these fascinating properties of PVDF can be used for device applications it was thought worthwhile to investigate its low frequency ac conductivity and dielectric relaxation behavior because very few data on dielectric relaxation are available in literature [11,12,15–18]. Moreover, the detailed studies on the mechanism of low frequency ac conduction and dielectric relaxation behavior are lacking. It is significant to mention here that the form (α-, β-, γ-, δ-, and mixture of these forms, etc.) and film processing methods of PVDF materials for device applications are also very important. In the past, many techniques such as injection molding, die-casting, hot rolling, etc. have been employed for the preparation of thick films of polymeric materials. These techniques, however, require sophisticated and costly equipment and large amount of raw materials. Further, with the earlier techniques it was difficult to obtain as-grown virgin films without strain since mechanical stress on the raw material is invariably applied while using the above techniques. Such strains may induce peculiar behavior of the dielectric and piezoelectric properties [19] in materials such as PVDF having high molecular weight (∼140,000) and P(VDF–CTFE). The solution evaporation technique used in the present studies is free from the effect described above. Further, it has many advantages viz.; (i) films of any thickness (≥10 μm) can be prepared under any desired conditions of temperature, etc., (ii) the preparation of doped films is very easy and safe, and (iii) the films prepared are free from unwanted impurities.

Keeping all these in mind we studied the ac conduction behavior of solution grown PVDF films in their virgin (unstretched) and uniaxially stretched state. Before conducting ac measurements, PVDF matrix was characterized for their structural, morphological and thermal behaviors. Our investigation is an attempt to provide an exhaustive data on low frequency ac conduction and dielectric relaxation behavior of solution grown and uniaxially stretched PVDF films in the frequency range 0.1 kHz–10 MHz and in the temperature range 77–400 K.

2. Experimental procedure

PVDF in white powder form, obtained from M/s. Polysciences, Inc. USA, was dissolved in *N*,*N*-dimethylformamide (DMF). Films of PVDF having thickness ∼80–300 μm were prepared in vacuum oven at ∼353 K by keeping the different amounts of PVDF–DMF solution in separate flat petri-dishes for 6 h. These PVDF films were very smooth and translucent in nature. The films were uniaxially stretched at an elevated temperature ∼423 K by using a specially designed stretching device. Fourier transform infra-red (FT-IR) investigation of both stretched and unstretched PVDF has been performed using Perkin–Elmer FT-IR Spectrometer. Change in PVDF morphology/phases has been observed by Leo 440 scanning electron microscope. Thermal analysis (DSC) has been performed on Mettler Toledo Star System. The phase determination in PVDF matrices has been observed by D-8 Advanced X-ray Diffractometer (Bruker). The stretched films having thickness ∼25, 45 and 80 μm were cut into pieces and gold electrodes were vacuum evaporated on both the sides of these stretched and unstreched (thickness ∼85 μm) films making M–P–M sandwich structure. The ac conductivity [$\sigma_m(\omega)$], dielectric constant [$\varepsilon'(\omega)$] and dielectric loss [$\varepsilon''(\omega)$] were measured using a GR 1615 A Capacitance Bridge in the frequency range 0.1 kHz–100 kHz and by HP 4192 A LF Impedance Analyzer in the frequency range 0.1 kHz–10 MHz in a specially designed three terminal cell in the temperature region 77–400 K. The dc conductivity was measured using Keithley's 617 electrometer and 2000 DMM.

3. Results

3.1. Structural, morphological and thermal characterization

Fig. 1 shows the FT-IR spectra of solution grown (unstretched) (Fig. 1 (a)) and uniaxially stretched (Fig. 1(b)) PVDF films. The entire characteristic vibronic bands before stretching (431.9, 481.6, 510.4, 601.6, 772.5, 838.1 and 878.1 cm^{-1}) and after stretching (411.6, 444.4, 487.7, 532.2, 613.5, 763.7, 796.1, 839.4, 879.3 and 975.9 cm^{-1}) and its comparison with reported values [12] indicates that PVDF (of present work) before stretching is in α-form and after stretching a mixture of α- and β-forms exists in the polymer matrix wherein α-form is in majority. Other notable observations from Fig. 1(a,b) are: (i) the peaks are more prominent/intensified in stretched film, (ii) a new peak at 975.9 cm^{-1} has appeared in stretched film, (iii) peak at 772.5 cm^{-1} of solution grown film split into two peaks at 796.1 and 763.7 cm^{-1}, and (iv) all peak positions of solution grown film shifted to correspondingly higher wave number in spectrum of stretched film. These facts indicate that the polymeric chains are more packed and forming crystals of PVDF when film was stretched without significant changes into polymer phases. Once molecules are more tightly packed it requires more energy to vibrate and hence resultant vibronic peaks shifted to higher wave number. Thus, all these observations indicate that in a stretching process (at specified stretched conditions employed in this study) amorphous matrix of solution grown PVDF film gets transformed into more ordered matrix which indeed was observed in its morphology discussed later in this paper.

As can be seen from the spectra of solution grown and stretched PVDF films, they both show similar vibronic bands except slight changes in peak positions. It can be inferred that in stretching process, form of PVDF matrix does not change and the polymer remains largely in the α-form. Only

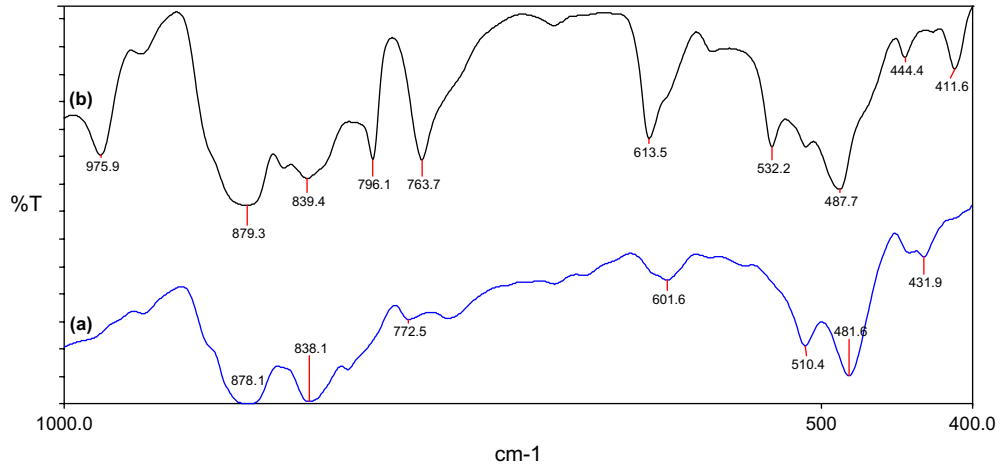

Fig. 1. FT-IR spectra of solution grown (unstretched) and uniaxially stretched PVDF films: (a) blue curve shows vibronic bands of solution grown PVDF (translucent) film and (b) gray curve shows vibronic bands of uniaxially stretched PVDF (transparent) film. (For interpretation of the references to colour in this figure legend, the reader is referred to the web version of this article.)

change at a given condition is the ordering of the matrix. Thus, from the various vibronic peak positions of both solution grown and stretched PVDF films, it is clear that the PVDF employed in the present investigation is mainly in α-form (mixture of α- and β-forms with α-form in majority) [12].

As per the conditions of the preparation of PVDF films we believe that in our case materials exist predominantly in α-form when the film is in unstretched form and in crystallized α-form when the film is stretched [12]. The dominance of the α-form of PVDF has been further confirmed by X-ray diffraction studies of unstretched film. Intense peaks at $2\theta \cong 17.8°$, 18° and 20° correspond to (100), (020) and (021) reflections, respectively, indicating α-form (in majority) and a diffuse peak around $2\theta \cong 20.8°$ corresponding to (110) and (200) reflections of β-form (in minority). These results are in agreement with previously reported [12] values; for α-form ($2\theta \cong 17.7°$, 18.4° and 19.9° and β-form $2\theta \cong 20.3°$).

Fig. 2(a,b) shows the scanning electron micrographs of solution grown and uniaxially stretched PVDF films, respectively. It is evident from these micrographs that significant number of crystallites has been formed upon uniaxial stretching of PVDF film. It confirms the observation regarding the phase transformation of PVDF into more ordered phases upon film stretching at the conditions employed in the present

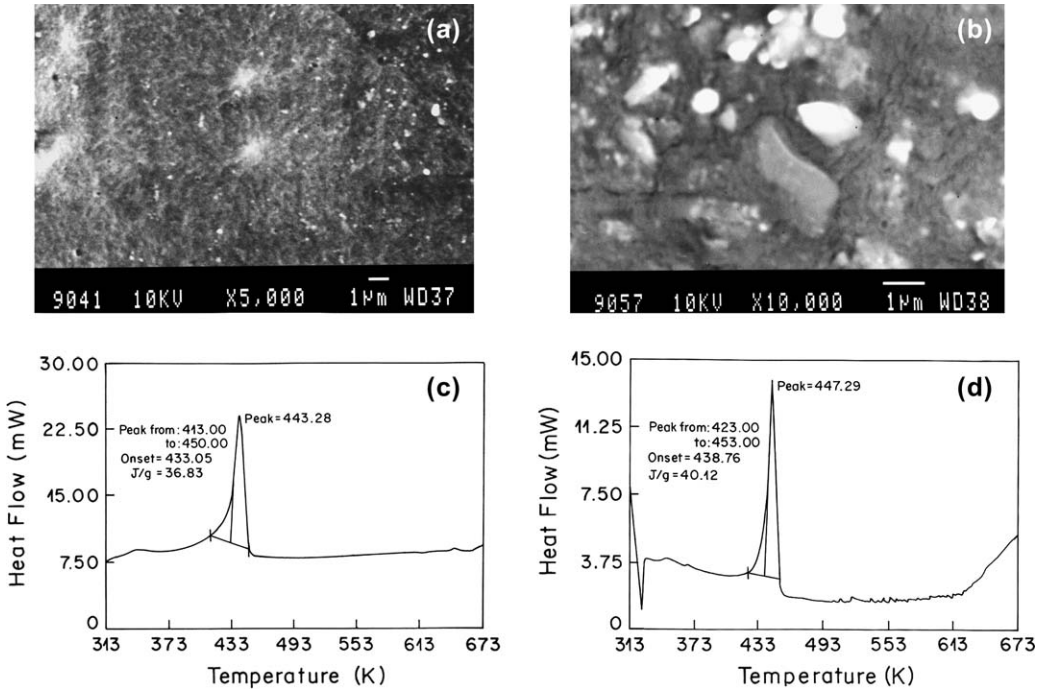

Fig. 2. Scanning electron micrographs (SEM) and differential scanning calorimetric (DSC) spectra of solution grown (unstretched) and uniaxially stretched PVDF films: (a) SEM of solution grown (unstretched) PVDF film having largely amorphous features; (b) formation of PVDF crystals in uniaxially stretched PVDF film; (c) and (d) DSC curves of solution grown (unstretched) and uniaxially stretched PVDF films.

study. Thus, stretching of the film produces PVDF in crystallized α-form. This is further supported by thermal behavior of these two types of PVDF films as shown in Fig. 2(c,d).

Fig. 2 (c) shows the DSC thermogram of solution grown PVDF film recorded as a function of temperature in the range 313–673 K at the rate of 20 K/min scan rate under nitrogen atmosphere. It shows endothermic peak at 443.28 K. This endothermic peak is associated with melting of the polymer having an enthalpy change of 8.811 cal/g. The sharp melting suggests the semi-crystalline nature of the polymer. At the same time the DSC thermogram (Fig. 2(d)) of uniaxially stretched PVDF film shows single endothermic peak at 447.29 K associated with the melting phenomenon. This peak is even sharper than the peak obtained for unstretched PVDF film (Fig. 2(c)) and shifts to the higher temperature side. Enthalpy change associated with the melting of stretched PVDF film suggests the increase in the crystallinity of the polymer as a result of uniaxial stretching. According to Nakagawa and Ishida [20], the percentage of crystallinity can be calculated from the ratio of enthalpy associated with the melting curve to the enthalpy of fusion of fully crystalline polymer, which is 25 cal/g. On this basis, unstretched PVDF film shows 35.24% crystallinity while upon uniaxial stretching this crystallinity has been increased to 39.83%. This clearly indicates that there is an increase in crystallinity after uniaxial stretching of the polymer.

3.2. Electrical characterization

The ac conductivity [$\sigma_m(\omega)$], dielectric constant [$\varepsilon'(\omega)$] and dielectric loss [$\varepsilon''(\omega)$] of solution grown (thickness ~85 μm) and uniaxially stretched (thickness ~25, 45 and 80 μm) PVDF films have been measured in the temperature range 77–400 K and in the frequency range 0.1 kHz–10 MHz and the results are presented in the following section. The dielectric parameters were evaluated by measuring equivalent parallel capacitance C_p and dissipation factor tan δ or the equivalent resistance R_p of the samples. A frequency dependent complex conductivity can arise from interfacial polarization at contacts, grain boundaries or from other inhomogeneities present in the system. The evidence for such effects arising from ohmic and nonohmic contacts has been discussed earlier [21,22]. The dielectric parameters are usually represented in terms of dielectric constant $\varepsilon'(\omega)$ and loss $\varepsilon''(\omega)$. In the past decades, especially in the interpretation of the data of amorphous materials [23], it has been customary to represent the data in terms of the dielectric constant $\varepsilon'(\omega)$ and $\sigma(\omega)$. Here, $\sigma(\omega)$ is the real part of the conductivity and is related [23,24] to dielectric loss as

$$\sigma(\omega) = \omega e_0 \varepsilon''(\omega), \tag{1}$$

where e_0 is free space permittivity and $\omega = 2\pi f$, f being the frequency. In the present investigation these parameters have been used to represent the observed experimental data. In an ideal insulator there are no free charges and $\varepsilon''(\omega)$ or $\sigma(\omega)$ is related only to the bound charges or the charges hopping between well defined sites, without contributing anything to long range motion or dc conductivity. However, in real material there are also some free charges, which give rise to dc conductivity without contributing anything to dielectric polarization. Hence, the measured ac conductivity $\sigma_m(\omega)$ will have the contribution from both ac and dc conduction and we can express [23–25] $\sigma_m(\omega)$ as

$$\sigma_m(\omega) = \sigma(\omega) + \sigma_{dc}, \tag{2}$$

where $\sigma(\omega)$ denotes the ac conductivity and σ_{dc} the dc conductivity. All these parameters discussed above have been used to represent and analyze the experimental data of the present investigation.

3.2.1. Temperature variation of ac conductivity [$\sigma_m(\omega)$], dielectric constant [$\varepsilon'(\omega)$] and dielectric loss [$\varepsilon''(\omega)$] at fixed frequencies

Fig. 3 shows the variation of ac conductivity [$\sigma_m(\omega)$] as a function of temperature in the range 77–400 K at four fixed frequencies; 0.1, 1, 10 and 100 kHz for uniaxially stretched PVDF films having three different thicknesses (~25, 45 and 80 μm). It is evident from Fig. 3 that in the low temperature region the measured ac conductivity $\sigma_m(\omega)$ is considerably higher than the dc conductivity σ_{dc} and it increases with increase in frequency. It shows a very weak dependence on temperature in the low temperature region, however, at high temperatures, $\sigma_m(\omega)$ becomes equal to σ_{dc} [22] and the temperature at which $\sigma_m(\omega)$ becomes equal to σ_{dc} increases with increase in frequency.

Fig. 4 shows the variation of dielectric constant $\varepsilon'(\omega)$ as a function of temperature in the range 77–400 K at four fixed frequencies 0.1, 1, 10 and 100 kHz for uniaxially stretched PVDF films having three different thicknesses (~25, 45 and

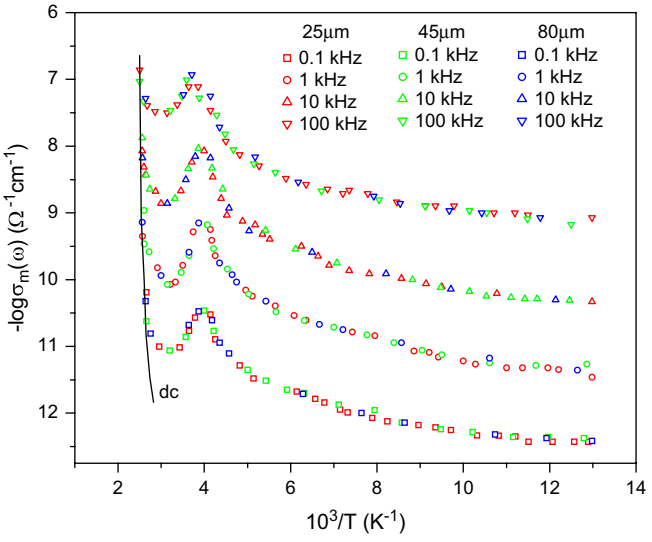

Fig. 3. Measured ac conductivity [$\sigma_m(\omega)$] as a function of reciprocal temperature at four fixed frequencies for three different; 25, 45 and 80 μm for uniaxially stretched PVDF films.

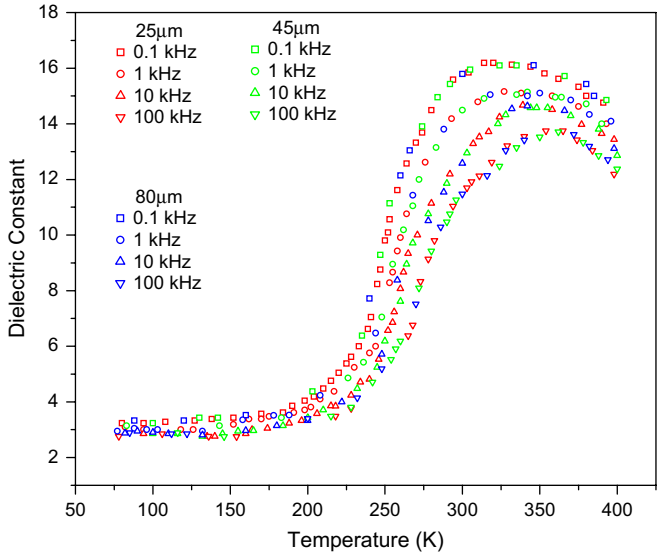

Fig. 4. Dielectric constant [$\varepsilon'(\omega)$] as a function of temperature at four fixed frequencies for three different thicknesses; 25, 45 and 80 μm for uniaxially stretched PVDF films.

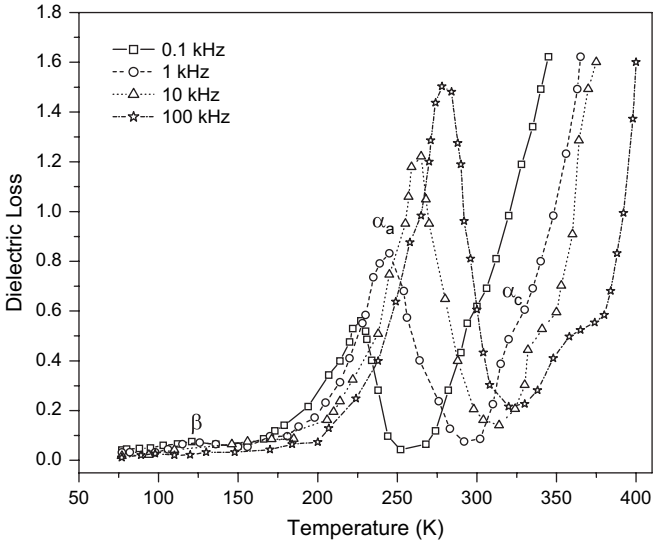

Fig. 5. Dielectric loss [$\varepsilon''(\omega)$] as a function of temperature at four fixed frequencies for solution grown (unstretched) PVDF film (thickness ~85 μm). The data have been taken from Ref. [17] for comparison with the present work.

80 μm). For a good electrode [21,22], $\varepsilon'(\omega)$ shows a peak when it is measured as a function of temperature. The possibility of a large barrier width giving rise to a small value of surface capacitance and a reasonable value of dielectric constant cannot be ruled out [21]. The barrier width is expected to be independent of the thickness of the sample. Hence, the value of dielectric constant shown at high temperatures for a fixed frequency should decrease with decreasing thickness provided the area of the sample is kept constant and the preparation conditions remain the same. It is evident from Figs. 3 and 4 that the $\varepsilon'(\omega)$ and $\sigma_m(\omega)$ are independent of thickness in the entire temperature region of measurement at all fixed frequencies indicating thereby that the measured values of dielectric constant and ac conductivity represent the true bulk behavior of the sample [26]. The thickness independent dielectric constant of the sample and a decrease of static dielectric constant with increasing temperature clearly indicate that the measured values of dielectric constant represents the true bulk phenomenon [27] and the electrode polarization and other spurious effects have negligible effects as has been observed earlier in case of vinyl chloride–vinyl acetate copolymer. It is also observed that the behavior of variation of $\varepsilon'(\omega)$ with temperature is similar for all the frequencies. At low temperatures $\varepsilon'(\omega)$ shows a little dependence on temperature, however, in the higher temperature region it shows strong temperature dependence and increases rapidly with increase in temperature at a given fixed frequency. This rapid increase in dielectric constant is followed by a slow decrease and thus giving a peak (Fig. 4). The temperature at which a peak in $\varepsilon'(\omega)$ is observed increases with increase in frequency. The peak value of dielectric constant is higher for low frequencies and lower for high frequencies. This behavior is consistent with a Debye-type dielectric dispersion characterized by a relaxation frequency f_0, where the measuring frequency is higher than f_0 in the low temperature region and lower at high temperatures than f_0.

Figs. 5 and 6 show the variation of dielectric loss $\varepsilon''(\omega)$ as a function of temperature in the range 77–390 K at four fixed frequencies; 0.1, 1, 10 and 100 kHz for solution grown film (thickness ~85 μm) and uniaxially stretched PVDF film (thickness ~25 μm), respectively. Three relaxations have been observed [17] for solution grown PVDF (Fig. 5) whereas for uniaxially stretched PVDF film (Fig. 6) only two relaxations are observed. The relaxations observed in the present investigation have been designated as the α_c-relaxation, the α_a-relaxation and the β-relaxation appearing from high temperature side to the low temperature side. It is evident from Figs. 5 and 6 that the high temperature side of the relaxation is masked by the dc conductivity and its magnitude increases with increase in frequency. The magnitude of α_a-relaxation

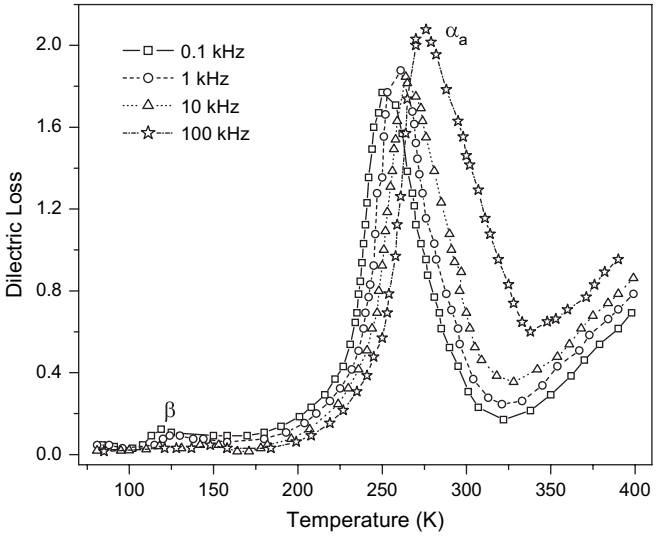

Fig. 6. Dielectric loss [$\varepsilon''(\omega)$] as a function of temperature at four fixed frequencies for uniaxially stretched PVDF film (thickness ~25 μm).

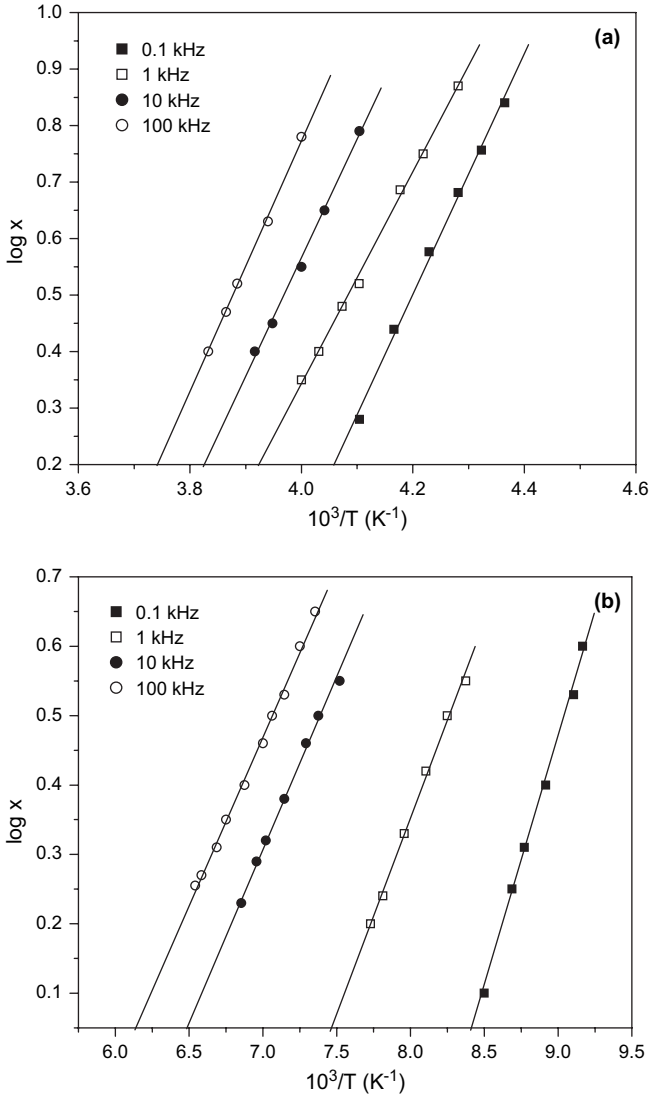

Fig. 7. $\log x$ versus reciprocal temperature plots for (a) α_a-relaxation and (b) β-relaxation for uniaxially stretched PVDF film (thickness ~25 μm).

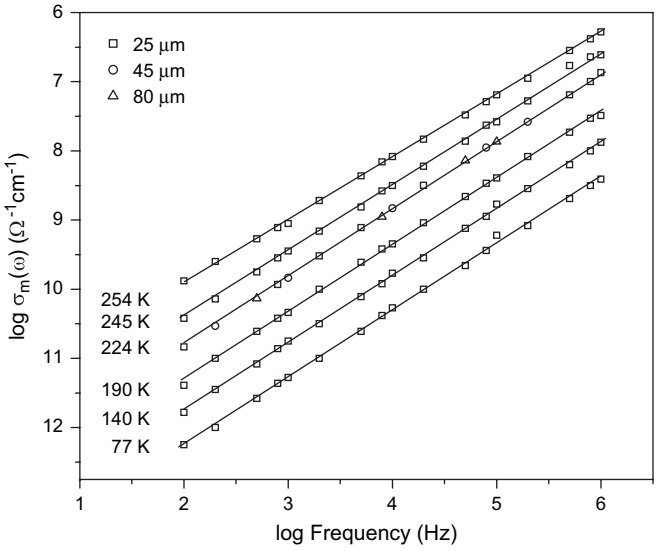

Fig. 8. Variation of measured ac conductivity [$\sigma_m(\omega)$] with frequency at different fixed temperatures for uniaxially stretched PVDF film (thickness ~25 μm). The data for three different thicknesses; 25, 45 and 80 μm are shown at 224 K.

increases with increase in frequency and shifts towards higher temperature side for higher frequencies. The β-relaxation (smaller in magnitude) appears in the low temperature side of the spectrum. The activation energy for these relaxations observed in $\varepsilon''(\omega)$ versus T plots (Figs. 5 and 6) has been evaluated by Fuoss approach [27,28] in which a variable x is defined as $x = [1+(1-K^2)^{1/2}]/K$, where $K = \varepsilon''/\varepsilon''_{max}$. The plot of $\log x$ as a function of $10^3/T$ plots (Fig. 7) gives a straight line and can be given by an empirical relation; $\log x = a + b/T$, where a is the intercept of the straight line on x-axis and b is the slope which gives the value of activation energy as $U = bk_B$ (eV), where k_B is the Boltzmann's constant. The values of activation energies obtained from the slopes of $\log x$ versus $10^3/T$ plots (Fig. 7) are given in Table 1.

3.2.2. Frequency variation of ac conductivity [$\sigma_m(\omega)$], and dielectric constant [$\varepsilon'(\omega)$] at fixed temperatures

As a representative result Fig. 8 shows the variation of measured ac conductivity $\sigma_m(\omega)$ as a function of frequency in the range 0.1 kHz–1 MHz at different fixed temperatures for uniaxially stretched PVDF film (~25 μm). Here, the values of measured ac conductivity for three different thicknesses (~25, 45, 80 μm) are shown at 224 K. It is observed [17] that for solution grown PVDF film (~85 μm), the value of slope s at 77 K is ~0.93 and is independent of temperature up to 200 K and then decreases with increase in temperature. For uniaxially stretched PVDF film, the value of slope s is ~0.97 at 77 K. This value is constant up to 224 K and then decreases with increase in temperature. It is also observed that at 77 K the measured ac conductivity shows an increase with increasing frequencies. This trend is also observed at higher temperatures.

Fig. 9 shows the variation of dielectric constant $\varepsilon'(\omega)$ as a function of frequency in the range 0.1 kHz–10 MHz at different fixed temperatures for uniaxially stretched PVDF film (~25 μm) as a representative result. Here, the measured values of dielectric constant for three different thicknesses

Table 1
The activation energy (W) calculated by Eq. (6), the range of activation energy (U) for the α_c-, the α_a- and the β-relaxations and activation energy (U) at 77 K for solution grown (unstretched) [17] and uniaxially stretched PVDF films

Samples	W (eV)	$U(\alpha_c)$ (eV)	$U(\alpha_a)$ (eV)	$U(\beta)$ (eV)	U (at 77 K) (eV)
Solution grown PVDF film	0.57	0.232–0.474	0.189–0.226	0.052–0.068	0.02–0.05
Uniaxially Stretched PVDF film	1.99	–	0.190–0.200	0.043–0.064	0.02–0.04

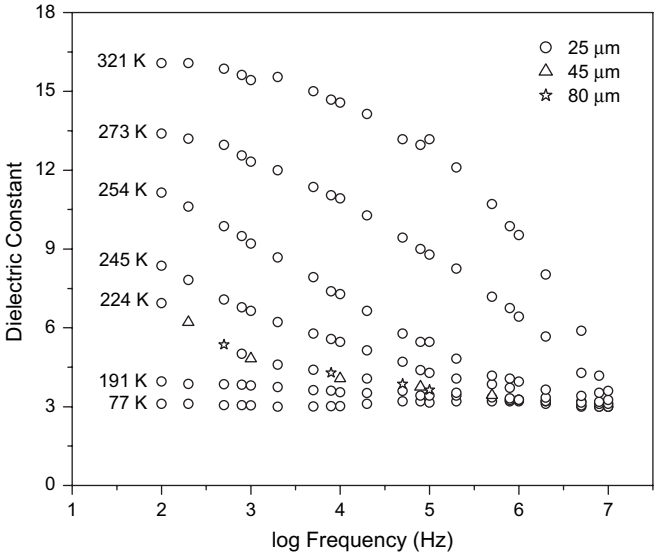

Fig. 9. Variation of dielectric constant [$\varepsilon'(\omega)$] with frequency at different fixed temperatures for uniaxially stretched PVDF film (thickness ~25 μm). The data for three different thicknesses; 25, 45 and 80 μm are shown at 224 K.

(~25, 45, 80 μm) are shown at 224 K. The dielectric constant at 77 K shows a very little dependence on frequency. However, at higher temperatures a rapid increase in dielectric constant is observed with decrease in frequency. It is evident from this figure that a frequency independent region for $\varepsilon'(\omega)$ is observed in the low frequency region at higher temperatures. However, this region could not be observed at all the temperatures because of the limitation of the measuring instrument.

4. Discussion

4.1. Low temperature region

At low temperatures a frequency dependent conductivity described [24] by

$$\sigma(\omega) = A\omega^s, \tag{3}$$

is observed where the exponent s is observed to be less than unity. The values of measured ac conductivity at 0.1, 1, 10 and 100 kHz at 77 K are given in Table 2. In the low temperature region, i.e. at 77 K where $\sigma_m(\omega) \gg \sigma_{dc}$, the variation of $\sigma_m(\omega)$ as a function of frequency can be expressed in terms of Eq. (3). The values of parameter s is ~0.93 for solution grown PVDF and ~0.97 for uniaxially stretched PVDF [17] films at 77 K and are independent of temperature up to 200 K for former and 224 K for latter, respectively, and beyond this temperature region it decreases with increase in temperature. The activation energy (U) for the charge carriers calculated at 77 K for these samples are given in Table 1, which provides the evidence of electronic hopping conduction [29] in these systems at low temperatures. An estimate of the density of states near the Fermi level $N(E_F)$ could be made from the ac conductivity $\sigma(\omega)$ at low temperatures by using Austin and Mott [30] relation given as

$$\sigma(\omega) = (1/3)\pi e^2 k_B T[N(E_F)]^2 \alpha^{-5} \omega[\ln(\upsilon_{ph}/\omega)]^4, \tag{4}$$

where the hopping near the Fermi level is expected to dominate. In Eq. (4), e is the electronic charge, k_B is the Boltzmann's constant, $\omega = 2\pi f$ is a frequency factor and α is the radius of the carrier wave function. Assuming $\upsilon_{ph} = 10^{13}$ Hz and taking the value of ac conductivity at 77 K and at 0.1, 1, 10 and 100 kHz, and taking the numerical value of α in the range 1–4 $Å^{-1}$, the values of $N(E_F)$ have been computed for different samples by using Eqs. (4) and (5), and are given in Table 2. The above equation is valid for uncorrelated hops between pairs of sites and the condition for which is given [30] by

$$[(4\pi/3)N(E_F)k_B T]^{1/3} > \alpha^{-1} \ln(\upsilon_{ph}/\omega), \tag{5}$$

This condition is satisfied for the value of α given in Table 2. The reasonable estimate of $N(E_F)$ from Eqs. (4) and (5) suggests that the charge carrier hopping near the Fermi level is between the nearest neighbor sites. In spite of the fact that Eq. (4) gives the reasonable estimate of $N(E_F)$, it fails to explain the temperature dependence of $\sigma(\omega)$. Eq. (4) predicts a linear temperature dependence of $\sigma(\omega)$, however, the measured values of ac conductivity show very weak temperature dependence in the low temperature region. Pollak [31] has argued that the temperature dependence of ac conductivity is due to multiple hops. However, it has been shown [32] that multiple hops cannot give strong temperature dependence of $\sigma(\omega)$ in transition metal oxide glasses. Pike [33] has tried to explain the temperature dependence of ac conductivity $\sigma(\omega)$ and the exponent s and suggested the following expression:

$$1 - s = 6k_B T/W_m, \tag{6}$$

where W_m is the activation energy and k_B is the Boltzmann's constant. Springett [34] and Elliott [35] have also suggested

Table 2
The measured ac conductivity $\sigma_m(\omega)$ at 77 K and density of states at Fermi level $N(E_F)$ computed by using Eqs. (4) and (5) assuming $\upsilon_0 = 10^{13}$ Hz and $\alpha = 1.0$, 2.0 and 4.0 $Å^{-1}$ at four fixed frequencies for solution grown (unstretched) PVDF [17] and uniaxially stretched PVDF films

Frequency (Hz)	Solution grown (unstretched) PVDF film				Uniaxially stretched PVDF film			
	$\sigma_m(\omega)$ at 77 K (Ω^{-1} cm^{-1})	$N(E_F)$ (10^{18} cm^{-3} eV^{-1})			$\sigma_m(\omega)$ at 77 K (Ω^{-1} cm^{-1})	$N(E_F)$ (10^{18} cm^{-3} eV^{-1})		
		$\alpha = 1.0$ $Å^{-1}$	$\alpha = 2.0$ $Å^{-1}$	$\alpha = 4.0$ $Å^{-1}$		$\alpha = 1.0$ $Å^{-1}$	$\alpha = 2.0$ $Å^{-1}$	$\alpha = 4.0$ $Å^{-1}$
100.0	2.51×10^{-13}	0.44	2.52	14.30	4.47×10^{-13}	0.59	3.37	19.05
1000.0	3.16×10^{-12}	0.62	3.48	19.70	5.25×10^{-12}	0.79	4.49	25.69
10,000.0	4.01×10^{-11}	0.98	5.52	31.22	5.62×10^{-11}	1.03	5.85	33.10
100,000.0	7.08×10^{-10}	1.15	8.50	48.12	7.94×10^{-10}	1.59	9.01	50.98

the similar temperature dependence of s. The number of pair centers responsible for ac conductivity can also be estimated by Pollak and Geballe [25] expression given for the frequency range 0.1–100 kHz in the following form:

$$\sigma(\omega) = (\pi/123)\left(e^2/k_B T\right)N_A N_D \Gamma(s/2)\Gamma(1-s/2) \times (\omega\tau)^s \tau^{-1}\left(11/\alpha^{-1}\right)^5, \quad (7)$$

The average value of τ in the frequency range 0.1–100 kHz has been taken [27,36] and a value of α as 4 Å^{-1}, with the known value of s and the measured value of ac conductivity $\sigma_m(\omega)$ at 77 K and 100 kHz has been used to estimate $N_A N_D$ from Eq. (7). The estimated value of $N = (N_A N_D)^{1/2}$ is of the order of 1×10^{18} cm^{-3} indicating a large number of donor and acceptor levels in this polymeric system. The estimated value of N seems to be reasonable and is in good agreement with the values reported [23,24] earlier for amorphous semiconductors.

The activation energy (W) calculated at 77 K using Eq. (6) for solution grown PVDF and uniaxially stretched PVDF films are higher than the activation energy (U) estimated at 77 K from ac measurement (Table 1). This shows that both Mott and Pike's model [24,33] give a qualitative picture and fail to give a quantitative agreement with the experimental results of the present investigation.

4.2. High temperature region where $\sigma_m(\omega)$ approaches σ_{dc}

The dielectric relaxation at high temperatures can be due to the following reasons: (i) electrode barrier [21,22] or surface effects [37] or macroscopic inhomogeneities [38], (ii) bulk effects: (a) micro-inhomogeneities [38,39]; (b) true bulk behavior (conventional Debye-type relaxation) [22,27,39]. Conclusive evidence whether the low frequency saturation dielectric constant or static dielectric constant ε_0 is due to surface barrier or due to bulk effects can be obtained by changing the thickness of the sample while keeping the area and preparation conditions of the sample same. Static dielectric constant (ε_0) will be independent of thickness for bulk effect and will decrease with decreasing thickness if it is due to a surface barrier capacitance [21]. Figs. 3 and 4 show $\sigma_m(\omega)$ and $\varepsilon'(\omega)$ independent of the sample thickness [26] representing the true bulk behavior of the sample.

It is evident from Fig. 8 that the decrease of slope s with increase in temperature is an outcome of the larger increase of conductivity with temperature at lower frequencies as compared to that at higher frequencies. At 77 K there is an evidence of dielectric dispersion in the low frequency region while at higher temperatures the dielectric constant shows a large dispersion (Fig. 9). The measured values of $\varepsilon'(\omega)$ at 224 K are independent of thickness and the scatter in the measured values is within the accuracy of measurement. This also suggests that the dielectric dispersion in this system is not due to the electrode polarization or surface barrier at the electrodes.

In the low temperature region the measured ac conductivity $\sigma_m(\omega)$ is almost independent of temperature and the strong temperature dependence occurs at higher temperatures for higher frequencies (Fig. 3). The nature of the temperature dependence of measured ac conductivity $\sigma_m(\omega)$ in the low temperature region makes it difficult to define a characteristic relaxation frequency f_0. However, in the high temperature region where $\sigma_m(\omega)$ approaches the dc conductivity σ_{dc}, the ac component of the conductivity may show a clearer evidence for f_0. In particular, the dielectric loss $\varepsilon''(\omega)$ derived from Eqs. (1) and (2) may show a Debye-type loss peak at $f = f_0$. Here, $\sigma(\omega)$ is the ac component of conductivity and e_0 is free space permittivity. A difficulty in this approach is that the magnitudes of $\sigma_m(\omega)$ and σ_{dc} are comparable at some temperatures (Fig. 3) and the uncertainty in the evaluation of $\varepsilon''(\omega)$ is large. Hence, it has been preferred to present the results in terms of $\varepsilon'(\omega)$ and $\sigma_m(\omega)$ and more emphasis has been given to $\varepsilon'(\omega)$ in interpreting the results in the temperature region where $\sigma_m(\omega)$ approaches σ_{dc}. It is, therefore, necessary to justify an analysis in terms of Debye-type dispersion.

The dielectric constant for a Debye-type process is given [40] as:

$$\varepsilon'(\omega) - \varepsilon_\infty = (\varepsilon_0 - \varepsilon_\infty)/\{1 + (f/f_0)\}^2, \quad (8)$$

where ε_0 and ε_∞ are the static and infinite frequency dielectric constants, respectively, f is the measuring frequency and f_0 is the relaxation frequency at which a peak in dielectric loss $\varepsilon''(\omega)$ is observed. In the low temperature region $f/f_0 \gg 1$ then $\varepsilon'(\omega) \to \varepsilon_\infty$ and at high temperature $f/f_0 \ll 1$, then $\varepsilon'(\omega) \to \varepsilon_0$. In the low temperature region the change in $\varepsilon'(\omega)$ with temperature is negligible and then it has a sharp rise at the temperature at which $f = f_0$. It can be observed that a strong temperature dependence starts at higher temperatures for higher frequencies or at lower temperature for lower frequencies indicating thereby that f_0 increases with an increase in temperature. It can be seen here that the region where there is a strong temperature dependence of $\varepsilon'(\omega)$ at a given frequency (Fig. 4) is the same at which $\sigma_m(\omega)$ approaches σ_{dc} (Fig. 3). Thus, the variation of $\varepsilon'(\omega)$ with temperature confirms the existence of loss peaks indicated in Fig. 3. The measured values of $\varepsilon'(\omega)$ at frequencies 0.1, 1, 10 and 100 kHz show a saturation region at high temperature end of the spectrum (Fig. 4) and this may be taken as an estimate of the static dielectric constant. The static dielectric constant has been estimated from the plots of dielectric constant versus temperature (Fig. 4) and the values have been plotted as a function of reciprocal temperature in Fig. 10(a). These values are in good agreement with the values of ε_0 achieved at higher temperatures in the dielectric constant versus frequency spectrum (Fig. 9). It is evident from Fig. 10(a) that ε_0 decreases with increase in temperature. Figs. 4 and 9 are consistent with Debye-type dispersion and suggest that the loss peaks depicted in Figs. 5 and 6 are real. The existence of well defined loss peaks has also been observed in vinyl chloride–vinyl acetate copolymer [27], polypyrrole, poly(*N*-methyl pyrrole) and their copolymers [41,42].

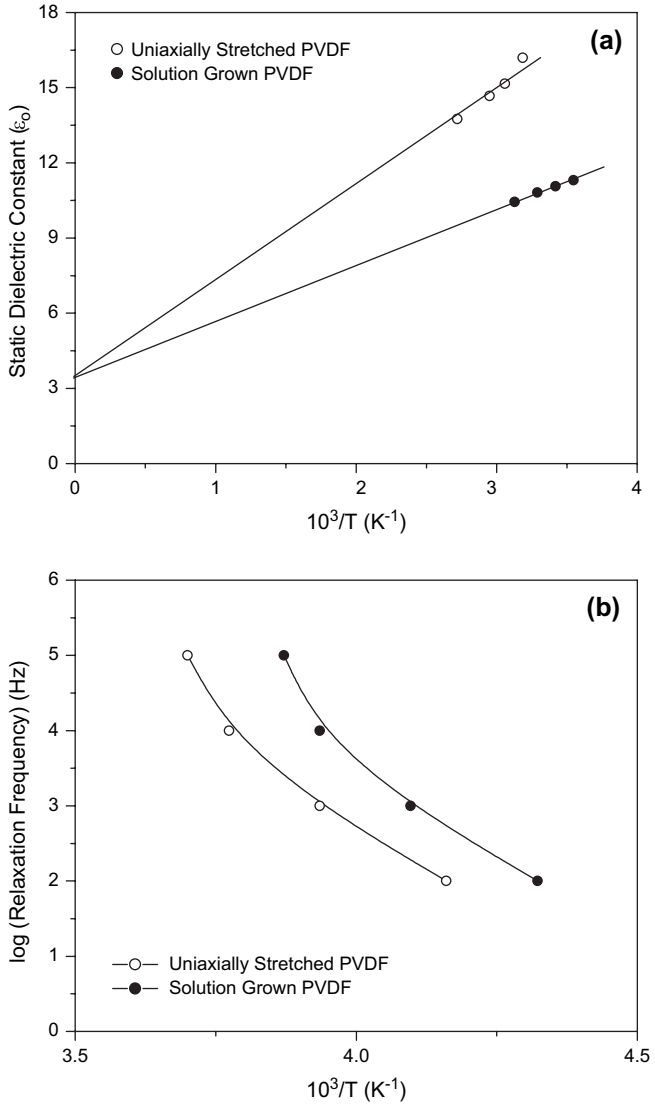

Fig. 10. (a) Static dielectric constant (ε_0) and (b) relaxation frequency (f_0) as functions of reciprocal temperature for solution grown (unstretched) PVDF (thickness ~85 μm) and uniaxially stretched PVDF (thickness ~25 μm) films.

The evaluation of relaxation frequency f_0 from ac conductivity measurements becomes difficult especially when the measurements have been made as a function of temperature. The alternative method for the determination of f_0 from the measured dielectric constant $\varepsilon'(\omega)$ versus temperature (Fig. 4) seems to be unrealistic. However, it does not have an ambiguity caused by the closeness of measured ac conductivity $\sigma_m(\omega)$ and dc conductivity σ_{dc} in the high temperature region (Fig. 3). It can be seen from Eq. (8) that if the temperature at which $\varepsilon'(\omega)-\varepsilon_\infty$ becomes equal to $(\varepsilon_0-\varepsilon_\infty)/2$ for a given frequency, the measuring frequency f becomes equal to the relaxation frequency f_0. The above discussion indicates that the well defined dielectric loss peaks have been observed in the temperature region where the measured ac conductivity $\sigma_m(\omega)$ approaches the dc conductivity σ_{dc} (Fig. 3). The relaxation frequency f_0 can be estimated from the measured dielectric constant $\varepsilon'(\omega)$ as a function of temperature or frequency (Figs. 4 and 9) and has been plotted in Fig. 10(b). The static dielectric constant ε_0 can also be determined from the measured frequency variation of dielectric constant $\varepsilon'(\omega)$ or temperature variation of dielectric constant $\varepsilon'(\omega)$ at fixed frequency. The estimated value of static dielectric constant ε_0 (Fig. 10 (a)) could at best be accurate within ±10%.

4.3. Dielectric relaxation behavior of solution grown and uniaxially stretched PVDF films

It is evident from Figs. 5 and 6 that there are three relaxations observed in solution grown PVDF film, however, only two relaxations are observed in uniaxially stretched PVDF film. These relaxations have been designated as the α_c-relaxation, the α_a-relaxation and the β-relaxation appearing from high temperature side to the low temperature side. It is interesting to note that the α_c-relaxation is absent in uniaxially stretched PVDF film (Fig. 6). It has already been reported [43] that the α_c-relaxation disappears on biaxial stretching of the PVDF films. The activation energy estimated [27,28] in the present investigation lies in the range 0.232–0.474 eV for the α_c-relaxation, 0.189–0.226 eV for the α_a-relaxation and 0.052–0.068 eV for the β-relaxation in case of solution grown PVDF film [17]. For uniaxially stretched PVDF film, the activation energy of the α_a-relaxation lies in the range 0.190–0.200 eV and for the β-relaxation it is 0.043–0.064 eV. The α_c-relaxation observed in the present investigation (Fig. 5) has been attributed to the molecular motions in the crystalline regions of the polymer main chain whereas the α_a-relaxation (Figs. 5 and 6) is associated with the micro-Brownian motion of the main polymer chain in the amorphous regions. In α-PVDF, two relaxations, i.e. the α_a- and the α_c-relaxations have been reported in the temperature region 233–278 K, where the former is due to the segmental motion of the main polymer chain associated with glass transition and the latter is due to changes in confirmation that can occur in the crystalline region of the polymer [13]. The β-relaxation observed in Figs. 5 and 6 is attributed to the rotation of the side group dipoles or to the local oscillations of the frozen main chains [44–46]. The electronic hopping conduction is dominant in the low temperature region in uniaxially stretched PVDF film. However, in the higher temperature region the dipolar relaxation process dominates over the electronic hopping mechanism.

5. Conclusions

The structural, morphological and thermal characterizations of solution grown (unstretched) and uniaxially stretched PVDF films show that PVDF matrix in unstretched form is largely amorphous and in α-form whereas in uniaxially stretched form, the PVDF matrix possesses large number of PVDF crystals and still retains the α-form in majority. The measured ac conductivity $\sigma_m(\omega)$ has been described by the relation $\sigma(\omega) = A\omega^s$, where the value of parameter s at 77 K is close to unity, which decreases with increase in temperature. The activation energy (U) estimated at 77 K gives indication

of electronic hopping conduction at low temperatures. Three relaxations, observed in the present work, have been designated as the α_c-, the α_a- and the β-relaxations appearing from high temperature side to the low temperature side. The α_c-relaxation is attributed to the molecular motions in the crystalline regions of the main polymer chain. The α_a-relaxation is associated with the micro-Brownian motion of the main polymer chain in the amorphous regions whereas the β-relaxation is attributed to the rotation of side group dipoles or to the local oscillations of the frozen main polymer chain.

Acknowledgements

The authors are grateful to Director, National Physical Laboratory, New Delhi for his permission to publish this work. One of us (R.D.P. Sinha) is thankful to the University Grant Commission, New Delhi for the award of a teacher fellowship.

References

[1] McCrum NG, Read BE, Williams G. Anelastic and dielectric effects in polymeric solids. London: John Wiley & Sons; 1967.
[2] Tashiro K. Ferroelectric polymers – chemistry, physics and applications. In: Nalwa HS, editor. New York: Marcel Dekker; 1995. p. 63.
[3] Kepler RG. Ferroelectric polymers – chemistry, physics and applications. In: Nalwa HS, editor. New York: Marcel Dekker; 1995. p. 183.
[4] Sessler GM, editor. Electrets. 3rd ed. Morgan Hill: Laplacian; 1999.
[5] Lovinger AJ. Science 1983;220:115.
[6] Eberle G, Schmidt H, Eisenmenger W. IEEE Trans Dielectr Electr Insul 1996;3:624.
[7] Sessler GM, Das-Gupta DK, DeReggi AS, Eisenmenger W, Furukawa T, Giacometti JA. IEEE Trans Dielectr Electr Insul 1992;27:872.
[8] Furukawa T. Phase Transitions 1989;18:143.
[9] Kawai H. Jpn J Appl Phys 1969;8:975.
[10] Kobayashi M, Tashiro K, Tadokoro H. Macromolecules 1975;8:161.
[11] Gregorio Jr R, Capito RC. J Mater Sci 2000;35:299.
[12] Gregorio Jr R, Ueno EM. J Mater Sci 1999;34:4489.
[13] Bello A, Laredo E, Grimau M. Phys Rev B 1999;60:12764.
[14] Platte M. Ferroelectrics 1987;75:327.
[15] Miyamoto Y, Miyaji H, Asai K. J Polym Sci Part B Polym Phys 1980;18:597.
[16] Koizumi N, Haikawa N, Babuka H. Ferroelectrics 1984;57:99.
[17] Singh R, Sinha RDP, Kaur A, Kumar J. Ferroelectrics 2005;329:91.
[18] Osaki S, Kotaka T. Ferroelectrics 1981;32:1.
[19] Wada Y, Hayakawa R. Jpn J Appl Phys 1976;15:2041.
[20] Nakagawa K, Ishida YJ. J Polym Sci Polym Phys Ed 1973;11:2153.
[21] Simmons JG, Nadkarni GS, Lancaster MC. J Appl Phys 1970;41:538.
[22] Singh R, Tandon RP, Panwar VS, Chandra S. J Appl Phys 1991;69:2504.
[23] Sayer M, Mansingh A, Reyes JM, Rosenblatt G. J Appl Phys 1971;42:2857.
[24] Mott NF, Davis EA. Electronic processes in non-crystalline materials. London: Oxford University Press; 1979.
[25] Pollak M, Geballe TH. Phys Rev 1961;122:1742.
[26] Mansingh A, Singh R, Sayer M. J Phys Chem Solids 1984;45:79.
[27] Singh R, Panwar VS, Tandon RP, Gupta NP, Chandra S. J Appl Phys 1992;72:3410.
[28] Fuoss RM. J Am Chem Soc 1939;61:234. 1941;63:369.
[29] Jonscher AK. Thin Solid Films 1967;1:213.
[30] Austin IG, Mott NF. Adv Phys 1969;18:41.
[31] Pollak M. Phys Rev 1964;133:A564; Pollak M. Philos Mag 1971;23:519.
[32] Mansingh A, Tandon RP, Vaid JK. J Phys Chem Solids 1975;36:1267.
[33] Pike GE. Phys Rev B 1972;6:1572.
[34] Springett BE. J Non-Cryst Solids 1974;15:179.
[35] Eliott SR. Philos Mag B 1971;36:1291; Eliott SR. Philos Mag B 1978;37:553.
[36] Mansingh A, Vaid JK, Tandon RP. J Phys C 1975;8:1023.
[37] Mansingh A, Srivastawa KN, Singh B. J Phys Chem Solids 1979;40:9.
[38] Tomazawa M. In: Tomozawa M, Doremus RH, editors. Treatise on materials science and technology, vol. 12. New York: Academic Press; 1977. p. 283.
[39] Macedo PB, Moynihan CT, Bose R. Phys Chem Glasses 1972;13:171.
[40] Hill NE, Vaughen WE, Price H, Davis M. Dielectric properties and molecular behavior. London: Van Nostrand; 1969.
[41] Singh R, Narula AK, Tandon RP, Mansingh A, Chandra S. J Appl Phys 1996;80:985.
[42] Singh R, Narula AK, Tandon RP. Synth Met 1996;82:63.
[43] Ishida Y. J Polym Sci A-2 1969;7:1835.
[44] Nakagawa K, Ishida Y. J Polym Sci Polym Phys Ed 1973;11:1503.
[45] Yano S, Tadano K, Aoki K. J Polym Sci Polym Phys Ed 1974;12:1875.
[46] Samara GA. J Polym Sci Polym Phys Ed 1989;27:39.